ISSN 1677-5090 impresso ISSN 2236-5222 digital © 2025 Revista de Ciências Médicas e Biológicas

DOI 10.9771/cmbio.v24i1.65969

Assessment of the spectral changes in root dentin after irrigation with chlorhexidine: a Raman spectroscopy study

Avaliação das alterações espectrais na dentina radicular após irrigação com clorexidina: um estudo por espectroscopia Raman

Fabiola Bastos de Carvalho¹, Hannah Barros², Isabele Cardoso Vieira De Castro³, Luiz Guilherme Pinheiro Soares⁴, Landulfo Silveira Júnior⁵, Antônio Luiz Barbosa Pinheiro⁶

¹PhD, Associate Professor, Center of Biophotonics, School of Dentistry, Federal University of Bahia, Salvador, Bahia, Brazil, ²PhD Student, School of Dentistry, Federal University of Bahia, Salvador, Bahia, Brazil, ³PhD, Center of Biophotonics, School of Dentistry, Federal University of Bahia, Salvador, Bahia, Brazil, ⁴PhD, Center of Biophotonics, School of Dentistry, Federal University of Bahia, Salvador, Bahia, Brazil, ⁵PhD, Professor, Center for Innovation, Technology and Education - CITE, Anhembi Morumbi University, Parque Tecnológico de São José dos Campos, São José dos Campos, São Paulo, Brazil, ⁶PhD, Full Professor, Center of Biophotonics, School of Dentistry, Federal University of Bahia, Salvador, Bahia, Brazil

Abstract

Introduction: Chlorhexidine (CHX) is a cationic biguanide that binds to negatively charged dentin molecules being slowly released (substantivity), thereby providing a long-lasting antimicrobial action. The aim of this study was to evaluate the spectral changes in the root dentin due to the presence of CHX used as an irrigant by means of Raman spectroscopy. Methodology: twenty human canine teeth were selected and divided into four groups according to the irrigation solution used. After biomechanical preparation, the roots were longitudinally sectioned for scanning by a Raman spectrometer (785 nm, 300 mW, 4 cm² resolution). Raman spectra were collected at six points along the root canal immediately (0 h), 24 h, 48 h, 72 h and 7 days after preparation. Results: the statistical analysis (ANOVA GLM) was applied to the principal component analysis (PCA) scores. Group CHX showed a strong change in the position of the phosphate hydroxyapatite band at ~963 cm², with a shift to higher wavenumbers for the time t = 0; as time passed this band shifted back to ~963 cm². This wavenumber shift in this ~963 cm² peak can be attributed to the presence of remnant CHX up to 7 days after root irrigation. For the Group CHX + Water, the shift to higher wavenumber was slight and maintained up to t = 72 h. Conclusion: Raman spectroscopy could detect the spectral changes caused by the CHX in the root dentin, thus representing an additional tool for identifying the adsorption of this compound after root canal preparation.

Resumo

Introdução: a clorexidina (CHX) é uma biguanida catiônica que se liga a moléculas de dentina carregadas negativamente, sendo liberada lentamente (substantividade), proporcionando assim uma ação antimicrobiana duradoura. O objetivo deste estudo foi avaliar as alterações espectrais na dentina radicular devido à presença de CHX usada como irrigante por meio de espectroscopia Raman. Metodologia: vinte dentes caninos humanos foram selecionados e divididos em 4 grupos de acordo com a solução de irrigação utilizada. Após o preparo biomecânico, as raízes foram seccionadas longitudinalmente para varredura por um espectrômetro Raman (785 nm, 300 mW, resolução de 4 cm²). Os espectros Raman foram coletados em seis pontos ao longo do canal radicular, imediatamente (0 h), 24 h, 48 h, 72 h e 7 dias após o preparo. Resultados: a análise estatística (ANOVA GLM) foi aplicada aos escores da análise de componentes principais (ACP). O grupo CHX apresentou forte alteração na posição da banda da hidroxiapatita fosfatada em ~963 cm², com deslocamento do pico para direita no tempo t = 0; com o decorrer do tempo, esse pico retornou para ~963 cm². Esse deslocamento do pico para direita no tempo t = 0; com o decorrer do tempo, esse pico retornou para ~963 cm². Esse deslocamento do pico para direita foi pouco pronunciado e mantido até t = 72 h. Conclusão: a espectroscopia Raman pode detectar as mudanças espectrais causadas pela CHX na dentina radicular, representando assim uma ferramenta adicional para identificar a adsorção deste composto após a instrumentação do canal radicular.

INTRODUCTION

The primary aim of root canal treatment of teeth with apical periodontitis is to disinfect the root canal system by using chemical and mechanical procedures

Palavras-chave: análise espectral raman; clorexidina; dentina.

Keywords: Raman spectral analysis; chlorhexidine; dentin.

Correspondente/ Corresponding: Fabiola Bastos de Carvalho – Endereço: Rua oito de dezembro 592 apt 201 Graça, Salvador – Bahia, Brasil. CEP 40.150-000 – E-mail: fabiolacarvalho@ufba.br

before filling the root canal. The persistence of infection in the root canal system and/or the periradicular area has been demonstrated as one of the causes of endodontic failures^{1,2}. The root canal instrumentation (manual or automated) is not fully effective as 10% to 80% of the radicular area is not touched by the instruments due to the complexity of the anatomy of the root canal system^{3,4}. To overcome this issue, irrigant solutions are being used as an adjuvant strategy along with instrumentation to reduce

the number and prevent the growth of microorganisms in the infected root canal, especially in areas unreachable to the instruments^{3,5,6}.

Different irrigation solutions such as sodium hypochlorite (NaOCl), chlorhexidine digluconate (CHX), 17% ethylene diamine tetracetic acid (EDTA) and citric acid has been used in endodontic treatments^{7,8}. NaOCl is the most used irrigation substance due to its antimicrobial action and capacity to dissolve organic tissue. Moreover, it has shown potential to be considered the main chemical in biomechanical preparation. On the other hand, CHX has been widely studied due to its broad spectrum of bactericidal action, as it can decrease gram-positive and gram-negative bacteria due to its low surface tension, thus efficiently entering infected dentinal tubules^{5,7}.

Unlike NaOCI, CHX has an adsorption capacity to dentinal calcium hydroxyapatite [HA]⁹. Because it is a cationic molecule, CHX binds with the negatively charged molecules of dentin, including the mineralised matrix and collagen matrix. As it is slowly released (substantivity), it provides long-lasting antimicrobial action¹⁰. Substantivity is one of the desirable characteristics of root canal irrigants, where the antimicrobial effects are desired for longer periods in cases of necrotic and infected pulp, thus promoting effective disinfection of the root canal system and contributing to the success of endodontic treatment ^{9,11}.

Different methods have been used for studying the adsorption of CHX into dentinal HA, including UV spectrophotometry^{12,13}, liquid chromatography¹⁴ and microbiological assays¹⁵. Raman spectroscopy is an optical

technique based on the measure of the light inelastic scattering from an incident monochromatic laser beam by biomolecules. It has been used to identify and analyse the chemical structure of these molecules¹⁶. These scattered photons are related to the vibrational energy of the molecular chemical bonds. Although the mechanism of Raman scattering (changes in the polarizability of the dipole induced by the electric field in the molecule) differs from that of infrared absorption (variation in the dipole moment occurring when the incident radiation coincides with the molecular vibration), both techniques provide information about the energy of the molecular vibrations¹⁶. The main applications include determination of the chemical structure of biomolecules¹⁷, quantitative evaluations in multicomponent mixtures¹⁸ and diagnosis of pathological changes in biological tissues and fluids^{19,20}.

Our team has used the Raman technique in various applications of non-invasive diagnosis of biological samples, such as detecting molecular changes in the osseointegration of dental implants²¹ and bone repair²², and in the effects on mineral and organic phases of bone repair when associating phototherapy with biomaterials²³. Therefore, this technique makes it possible to determine the nature and relative quantity of the biochemical compounds present in both normal and altered tissues due to pathological or regenerative processes. The important Raman peaks of the calcium hydroxyapatite (CHA) (mineral phase), as well as the collagen (protein—organic phase), are presented in Table 1. The CHX peaks (solid form) from the literature are also presented in Table 1.

Table 1 - Peak positions and attribution of the main Raman bands of basal bone used in the interpretation of the spectra of Figure 2. The CHX peaks from the literature are also shown.

Raman peak	Attribution	Importance	Bone	References
~429	v_2 out-of-plane stretching of phosphate apatite (PO $_4^{3-}$)		X	[24]
~453	v_2 out-of-plane stretching of phosphate apatite (PO $_4^{3-}$)		X	[24]
~592	v_4 stretching of phosphate apatite (PO $_4$ ³⁻) and COO ⁻ modes of collagen		X	[24, 25]
~670	C–Cl stretching – CHX			[26]
~854	C–C stretch of proline ring – collagen matrix	Higher intensity in collagen III compared with collagen I	X	[25, 27, 28]
~881	C–C stretch of proline/hydroxyproline ring – collagen matrix		X	[25, 27, 28]
~924	$C-COO^-$ skeletal backbone – collagen matrix	Higher intensity in collagen III compared with collagen I	X	[25, 27]
~958 to ~961	v_1 symmetric stretching of phosphate apatite (PO $_4^{3-}$)	Band position and bandwidth highly sensitive to carbonate substitution in the phosphate apatite. Band position at 956 cm ⁻¹ indicated an amorphous, highly carbonated bone; at 962 cm ⁻¹ indicated a high crystalline phosphate apatite. Smaller bandwidth indicates lower substitution of phosphate by carbonate in the apatite lattice (higher crystallinity). Higher bandwidth indicates smaller and unordered crystallites by carbonate substitution of phosphate. As bone matured, the size of the individual mineral crystal was found to increase	X	[28, 29]
~1002 to ~1010	Ring breathing mode – phenylalanine	Higher for collagen III compared with collagen I	X	[25, 27]

~1028 to ~1037	v_3 asymmetric stretching of phosphate apatite (PO $_4^{3-}$)		X	[30]
~1046	v_3 asymmetric stretching of phosphate apatite (PO $_4^{3-}$)			[30]
~1063	v_1 symmetric stretching CO_3^{2-} ion	carbonate hydroxyapatite		[31]
~1073	v_1 symmetric stretching B-type carbonate (CO $_3^{2-}$)	Substitution of the carbonate ion in the phosphate position in the hydroxyapatite lattice structure. Peak intensity increased with carbonate substitution	X	[28]
~1077	v_3 asymmetric stretching of phosphate apatite (PO $_4^{3-}$)	In carbonated apatites the band broadened and the peak shifted to lower wavenumbers. The overlap with the carbonate band at 1072 cm ⁻¹ could reduce the measurement precision even with lower carbonated apatites		[29]
~1093	СНХ			[32]
~1162	CH and NH modes of hydroxylysine, C–N stretch - collagen matrix		X	[25]
~1250 to ~1300	Amide III (C-N stretching/N-H bending) – collagen matrix	Depends on the side-chain structure of the protein; higher for collagen III compared with collagen I	X	[25, 27, 33]
~1268	Tautomeric forms formed from—CNH—NH—CNH— in protonated CHX; C—N stretching			[26, 34, 35]
~1323	CH deformation – collagen matrix	Higher for collagen I compared with collagen III	Χ	[25, 27]
~1345	CH ₂ wagging – collagen matrix	Higher for collagen III compared with collagen I	Χ	[25, 27]
~1428	CH ₂ deformation – collagen matrix	Present in collagen III	Χ	[25, 27]
~1450 to ~1460	CH ₂ /CH ₃ bending/wagging of methylene side chain – collagen matrix	Collagen I was the most abundant in mature bone. Its wavenumber was at around 1443 $\rm cm^{\text{-}1}$ for collagen I and changes to 1454 $\rm cm^{\text{-}1}$ for collagen III	X	[27, 28, 33]
~1564	NH ₂ deformation and C=N stretching from biguanine moiety – unprotonated CHX			[34, 35]
~1608	NH ₂ deformation and C=N stretching from biguanine moiety – protonated CHX			[34, 35]
~1667	Amide I (C=O stretch) – collagen matrix	This peak could change to 1675 cm $^{\text{-}1}$ in case of breakdown or rupture of collagen cross-link. Its wavenumber was at around 1660 cm $^{\text{-}1}$ for collagen I and changed to 1675 cm $^{\text{-}1}$ for collagen III	X	[27, 33]

Source: Survey data

It was hypothesised that the use of CHX could cause changes in the root dentin, which was detectable by Raman spectroscopy. This study aimed to evaluate, by means of Raman spectroscopy (785 nm) and principal component analysis (PCA), the spectral changes occurring in the phosphate and carbonate peaks of CHA (~960 and ~1070 cm⁻¹, respectively) and methyl and methylene peaks of collagen (~1460 cm⁻¹) in radicular dentin due to the presence of CHX used as an irrigation solution in root canal preparation.

METHODOLOGY

Sample Preparation

This study was approved by the local Research Ethics Committee (Protocol No. 608.937). It used 20 maxillary and/or mandibular canine teeth presenting the following characteristics: formed apexes, straight root, single root canal, without internal resorption and/or calcification and

without previous endodontic treatment. Internal anatomic characteristics were evaluated by radiographs taken in the mesiodistal direction. Teeth were cleaned with water and a curette to eliminate possible tissue reminders and were subsequently sterilised in an autoclave.

A carborundum disc (22.2 x 0.6 mm, Dentorium Inc., Farmingdale, New York, USA) was used for sectioning teeth at the cement-enamel junction as well as for creating longitudinal grooves on the vestibular and lingual surfaces of each tooth for cleavage after root canal preparation. The working length (WL) was performed by the visual method by placing a K-type file #15 (Dentsply Maillefer Inc., Ballaigues, Switzerland) in the root canal until it could be visualised in the apical foramen. It was withdrawn by 1.0 mm to establish the WL.

The sample was divided into four groups: experimental (CHX and CHX + Water) and control (Group A and Group B) (Table 2) with five teeth each. In the experimental groups, the root canals were prepared by the rotary

technique with the ProTaper® Universal System (Dentsply Maillefer Inc., Ballaigues, Switzerland) in the following operative sequence: S1, S2, F1, F2, F3, F4 and F5 to the WL, using an X-Smart[®] Motor (Dentsply Maillefer Inc.) of 250 rpm and 1.0 N/cm. In Group CHX, the teeth were prepared using 1.0 mL of 2.0 % CHX solution (FGM Ltda., Joinville, SC, Brazil) as an irrigant solution applied to each file change. In the Group CHX + Water, the teeth were also instrumented by using 1.0 mL of 2.0 % CHX solution (FGM Ltda., Joinville, SC, Brazil) as irrigant solution at each change of file; however, at the end of root canal preparation, they were rinsed with 1.0 mL of distilled water. In Control Group A, the teeth were instrumented according to the steps used in Group CHX. However, the irrigant solution used during the entire preparation was a volume of 1.0 mL of distilled water at each change of file. In Control Group B, the tooth was not instrumented; instead, it only cleaved through the vestibular and lingual grooves. The irrigation was performed for all groups with a disposable syringe and a needle (NaviTip 31ga; Ultradent, South Jordan, UT, USA) placed at the WL minus 1.0 mm.

Table 2 - Distribution of the study groups according to the irrigation solution used.

Groups	Irrigation protocol during instrumentation
Group CHX	CHX 2.0 % solution
Group CHX + Water	CHX 2.0 % solution + rinsed with distilled water
Control Group A	Distilled water
Control Group B	Uninstrumented teeth

Source: Survey data

After preparation, the root canals were dried with sterilised absorbent paper points F5 (Dentsply Maillefer Inc., Ballaigues, Switzerland). The teeth were then cleaved with a manipulation spatula, supported in the longitudinal grooves previously made, and the dentin walls of the root canals were submitted to Raman spectroscopy measures.

Raman spectroscopy

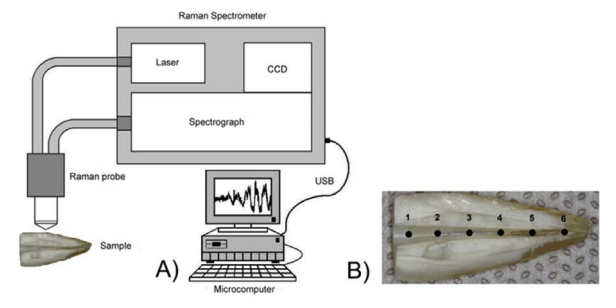
The Raman spectra of the root canals were obtained in the Raman Spectroscopy Laboratory of the Biophotonic Center of the School of Dentistry at the Federal University of Bahia. The dispersive Raman spectrometer (Figure 1A) was composed of a diode laser (785 nm excitation wavelength, 400 mW excitation laser output power; model BRM-785E, B&WTek Inc., Newark, DE, USA) and a dispersion spectrograph (model Shamrock 303i, Andor Technology Ltd., Belfast, Northern Ireland), with a diffraction grating of 600 lines/mm and resolution of 4 cm⁻¹, coupled to a back-illuminate, deep depletion CCD camera with 1024x128 pixels (model iDUS*, Andor Technology Ltd.) at a working temperature of -70 °C. The system uses a "Raman probe" fibre optic cable (model BAC102, BWTek Inc.) to excitation the sample and collect the Raman spec-

tra. The 1.5 m-long Raman probe cable is composed of an excitation fibre of 105 μ m and a collection fibre of 200 μ m in diameter, with a focal (working) distance of 10 mm.

The spectrophotometer response and calibration were verified before data collection using the spectrum of a tungsten lamp (for spectral response correction – ordinate axis) and the spectrum of naphthalene (for Raman shift calibration – abscissa axis). This correction/calibration was applied to the spectra before the data pre-processing procedure.

Spectra acquisition was performed by a microcomputer using the Solis* software (Andor Technology Ltd.), selecting an exposure time of 10 s (1 s, 10 accumulations) and laser power adjusted to 300 mW on the sample. This acquisition time and power caused no visible damage to the samples. The readouts were made at six points distributed along the root canal longitudinal axis (Figure 1B) from the cervical up to the apical region of the root in all the groups, with the probe's focal point at the dentin surface in all points. Raman spectra were collected immediately (0 h), 24 h, 48 h, 72 h and 7 days after root preparation.

Figure 1 - A) dispersive Raman spectrometer setup; B) instrumented root canal with the measured points highlighted.



Source: own authorship

After acquisition, the spectra were pre-processed and stored for later statistical analysis. Pre-processing consisted of manual removal of cosmic rays spikes and subtraction of the baseline fluorescence, where a 5th order polynomial function was adjusted in the spectral range between 400 and 1800 cm⁻¹ on the raw spectrum, and the polynomial (low-frequency component – fluorescence) was subtracted, revealing the high-frequency spectral components (Raman peaks). This pre-processing was performed using a routine written in the Matlab 7.01 program (The Mathworks Inc., Natick, MA, USA). After pre-processing, the spectra were normalised by the area under the curve and stored in ASCII format for later plotting and analysis. The ASCII data were imported into the Excel software, separated by experimental groups, and each tooth's mean spectra were obtained.

Principal component analysis (PCA) was carried out to provide a way to detect the spectral changes due to the presence of CHX and to correlate these changes to the time of action of the CHX on the radicular dentin of the root canal. For this purpose, the spectra of dentin of all groups in all time intervals were submitted to PCA (Matlab 7.01, The Mathworks Inc., statistics toolbox, princomp.m function). The principal component's output variables (loading vectors – PCs and scores) were evaluated, and the features were compared in each group. The PCs revealed the spectral changes that occurred in the main peaks of dentin in each group due to the presence of CHX and time of root exposure to CHX in terms of band intensity, position and bandwidth, and the scores intensities could relatively quantify these changes. PCA has been used with Raman spectroscopy to detect spectral changes in an experimental model of osteoarthritis tissue after low-level laser therapy²² and to model the risk of clinical complications related to diabetes and hypertension in urine samples³⁶.

Statistical analysis

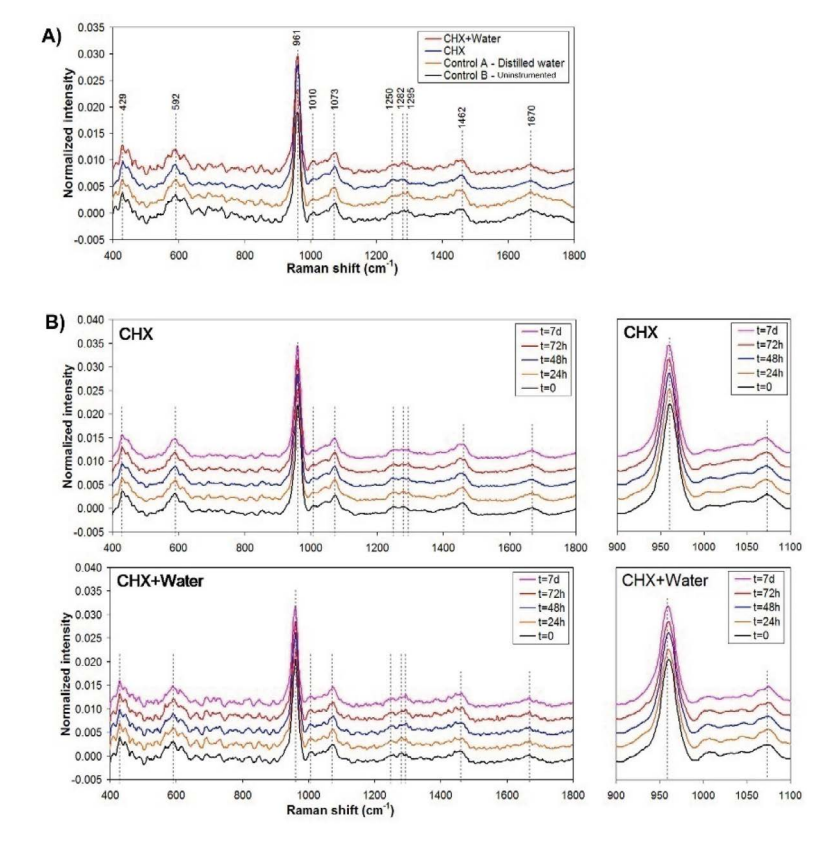
ANOVA general linear model (GLM) was applied to the PCA scores using Minitab 15.0 software (Minitab, Belo Horizonte, MG, Brazil). The data were initially analysed to verify their normality (Kolmogorov-Smirnov normality test). A two-way ANOVA analysis with a balanced design was conducted. Predictor variables were the treatment (CHX; CHX + Water; Control A and Control B) and the time interval (0 h, 24 h, 48 h, 72 h and 7 days after root canal preparation), which were transformed into a "dummy

variable". All testing was carried out with a significance level of 5 % (p < 0.05), and the adequacy of the models was evaluated with the adjusted R^2 .

RESULTS

Figure 2A presents the mean normalised Raman spectra of dentin from all groups at time t = 0. These spectra show general features of dentin, with peaks and attributions, as seen in Table 1. The comparison of the spectra at t = 0 suggests that Group CHX presented bands at ~961 and ~1,073 cm⁻¹ (phosphate and carbonate HA bands, respectively) with higher intensities when compared to the other groups. Figure 2B presents the mean normalised Raman spectra of dentin from the CHX and CHX + Water groups for the experimental times t = 0 h, 24 h, 48 h, 72 h and 7 days after root canal instrumentation. Also, it is plotted the region of the phosphate and carbonate HA bands (~961 and ~1,073 cm⁻¹, respectively). The spectra of both groups with and without distilled water presented the same general spectral features of dentin. They did not present remarkable differences depending on the time of CHX permanence after root canal preparation. Therefore, a more detailed analysis of these spectral changes (intensities, bandwidths and band positions) based on the spectral decomposition by PCA was performed to find and explain such differences.

Figure 2 - A) Raman spectra from dentin of the groups at t = 0. B) Raman spectra of dentin from the CHX and CHX + Water groups at different times t = 0 h, 24 h, 48 h, 72 h and 7 days after root canal preparation.



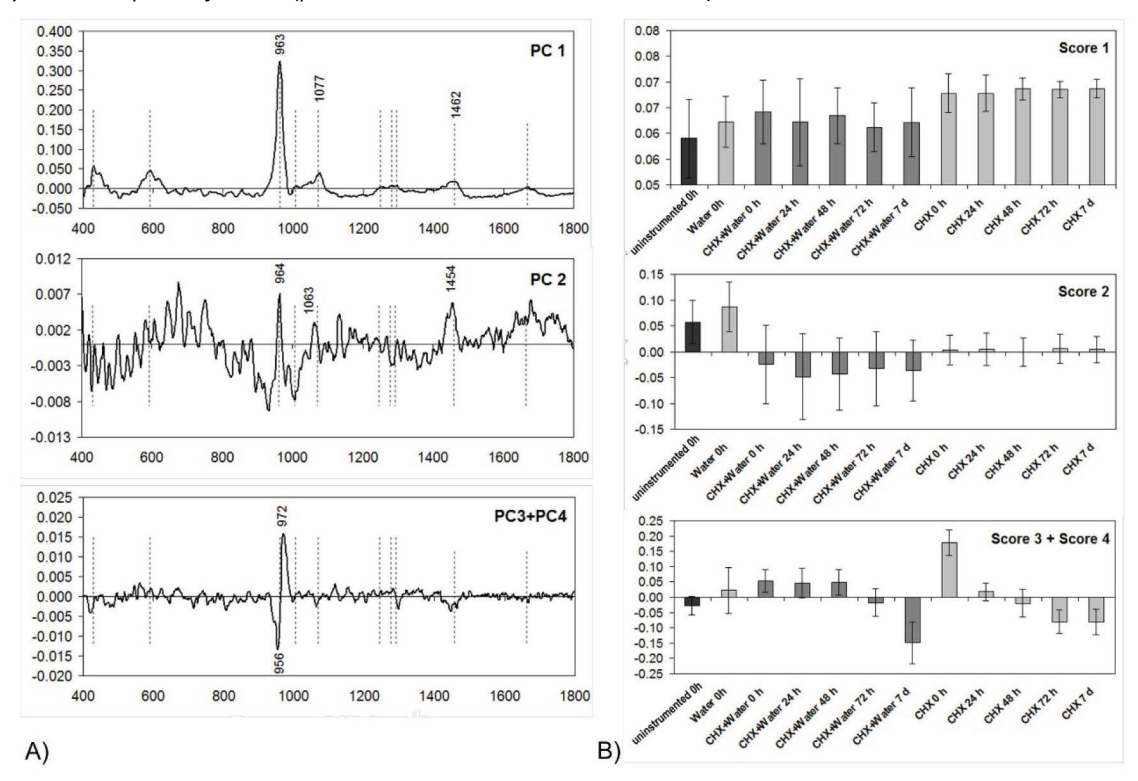
Source: own authorship

PCA has been employed to check the spectral differences induced by the presence of the CHX adsorbed over the surface of the dentin. Any spectral changes induced by CHX suggest that it is still present in the root canal and potentially acting as an antimicrobial agent. First, the PCs and scores were calculated, and the PCs were compared to the Raman spectra of the uninstrumented teeth (Figure 2A – Control B) to find any spectral features different from the dentin that could be attributed to the presence of CHX. Then, the scores that presented evidences of spectral differences in the Raman bands related to the CHA were plotted. The intensity information contained in these scores would indicate the presence of remnant CHX used in the irrigation that is still adsorbed over the dentin surface. Ultimately, this score may indicate its concentration, although this was not the aim of this study.

Figure 3A presents the first four PCA variables (PCs and scores) calculated using the Raman dataset. These components represent the most relevant spectral information presented in the whole dataset and account for more than 95% of the spectral variation. It is observed that PC1 presents the most spectral features common to dentin, with peaks of phosphate and carbonate HA and proteins. PC2 presents Raman features of phosphate HA

at ~963 cm⁻¹, carbonate HA at ~1,063 cm⁻¹ and methyl and methylene peaks of collagen at ~1,454 cm⁻¹. PC3 and PC4 present spectral features in the ~960 cm⁻¹ region, with a negative peak at the left and a positive at the right, indicating a peak shift to the higher wavenumber. Figure 3B presents the mean value of each experimental group's first four principal components scores at different times. Score 1 showed that Group CHX presented the same intensity at different times, with lesser variation compared to Group CHX + Water; this fact will be discussed in the next paragraphs. The Score2, which is attributed to phosphate HA and collagen, indicated that the Group CHX + Water had a reduced phosphate HA and collagen compared to the Control Groups A and B, and to a lesser extent for the Group CHX. Since the PC3 and PC4 present the same spectral features, the Score3 and Score4 were summed and indicated that the Group CHX had a strong change in the phosphate band at ~963 cm⁻¹. This band shifts to higher wavenumbers for the time t = 0, and as time passes, this phosphate band shifts back to ~963 cm⁻¹. For the Group CHX + Water, the shift to higher wavenumber occurred, but it was less pronounced and maintained shifted up to t = 72 h. At t = 7 days, the Group CHX + Water presented a very strong shift to a lower wavenumber.

Figure 3 - A) Plot of the first four principal components loading vectors (PC1 to PC4) obtained from the Raman dataset, indicating the spectral features relevant for the differentiation between the groups of root canals containing CHX. The vertical lines are in the same positions as the main peaks of instrumented dentin teeth (Control B) of Figure 2. B) Plot of the mean of the groups' first four principal components scores (Score1 to Score4). PC3 and PC4 and the respective Scores 3 and 4 were summed as they present closely the same spectral features (presented as PC3+PC4 and Score3+Score4).



Source: own authorship

/Statistical analysis was based on the analyses of Score1, Score2, and Score3+4. The hypotheses suggested for the changes in the spectrum are that the presence of cationic CHX would induce changes in the polarizability of the HA due to protonation with the anionic phosphate of dentinal HA. This change in the spectrum, characterised by a Raman shift of the phosphate HA band at ~960 cm⁻¹ to the right, suggested the presence of CHX.

Protonation, the addition of an H⁺ proton to an atom, molecule or ion, forms a conjugated acid. Protonation increases the mass and electric charge of a substrate, in addition to changing the hydrophilicity, reduction potential, optical properties and others. This is related to the acidity of the medium and is a reversible process. Considering the catalytic hydrogen model in which there would be adsorption of protons into negatively charged oxygen ions on the surface of orthophosphate groups found within apatites³⁷, the protonation process would result in a partial transformation of the PO_a into PO_a into PO_a groups^{38,39}. This superficial protonation of apatite would be intimately related to the hydrogen bonds, which tend to be increased with the reduction in pH (lower pH, greater protonation). Protonation would, therefore, be responsible for breaking the Ca-O bond and could explain the spectral changes observed in the present study; this, due to being reversible, could be the cause of the change in the position of the phosphate peak to ~960 cm⁻¹ and return to the previous state, due to the substantivity of CHX. The experiment was not capable of causing morphological changes in the HA crystals (dissolution), only changes in polarizability. Also, no Raman feature was observed in the scores associated with the adsorbed CHX.

With regard to Score1, there was a greater intensity in the Groups with CHX in all the experimental time intervals and in the Group CHX + Water 0 h, which suggested an increase in the polarizability of the molecule induced by CHX and that in the Groups without CHX and CHX + Water, after 24 h the polarizability returned to the values of the Group CHX + Water, which was higher than the value found in the Group Control B. Regarding the Score2 with features of carbonated HA (peak ~1,064 cm⁻¹) and collagen (peak at ~1,454 cm⁻¹), it may suggest changes in the polarizability with a consequent change in the carbonate peak at ~1,063 cm⁻¹ and collagen peak at ~1,464 cm⁻¹, less intense for the Group CHX + Water than for the Group CHX. Analysis of Score3+4 showed that there was a shift to the right of the phosphate HA peak to ~962 cm⁻¹, which was very intense for CHX at zero h, and that this peak returned to the original values (even further to the right than of Control B) after 7 days. The Group CHX + Water had different behaviours. For the time interval zero h up to 48 h, the shift of the peak ~964 cm⁻¹ was close to that of the Group Water. At 72 h, the peak shifted to the left, and in 7 days, the peak shifted to the right, with a smaller Raman shift also than the healthy dentin. This suggested that the water did not have a strong capacity to change the polarizability of HA in the time intervals of 48

h; however, at 7 days, there was a shift in the peak of HA to \sim 962 cm⁻¹ (shift to lower wavenumber) which suggests deprotonation of HA by the water (basification of dentin) or even carbonation.

To find which variable was responsible for the differences observed in the spectral changes, the ANOVA general linear model (GLM) was applied. The GLM shown in Table 3 allowed the authors to observe that the intensities of Score1, Score2, and Score3+4 presented statistically significant differences for the variable treatment of the canals. However, only Score3+4 was affected by the variable evaluation time interval after preparation.

Table 3 - Summary of the ANOVA GLM applied to the first four PCA scores.

PCA variable	Variable	Adjusted SS	F	<i>p</i> Value	
Score1	Time	0.000458	0.43	= 0.788	
	Treatment	0.0022744	28.35	< 0.001*	
Score2	Time	0.003850	0.34	= 0.848	
	Treatment	0.222063	26.43	< 0.001*	
Score3+4	Time	1.19212	87.58	<0.001*	
	Treatment	0.32031	31.37	< 0.001*	

^{*} Statistically significant differences (*p* < 0.05) Source: Survey data

DISCUSSION

Endodontic infection is characterised by the presence of microorganisms in root canal systems. Different antimicrobial agents may be used for disinfection; however, the time of action of irrigant substances is restricted to the biomechanical preparation procedure. Studies have demonstrated that CHX is capable of being adsorbed into the dentinal walls (substantivity), thus promoting a prolonged antimicrobial effect ^{5,9,12}.

The capability of Raman spectroscopy to detect the presence of CHX was confirmed by the analysis of the results from the groups rinsed with water (Group CHX + Water), which presented the shift in the phosphate bands nullified after 72 h. However, after 7 days, the Raman shift in this rinsed group was stronger than it was in the CHX group, suggesting deprotonation due to changes in the pH induced by the water (basification) or carbonation. The peaks of CHX were not directly observed; only the effect of its presence caused the band shifts.

Evaluation of the residual effect of CHX has been based on different approaches. Mahendra et al. ¹⁵ (2014) compared the antimicrobial substantivity of different concentrations of CHX used as irrigant solutions during biomechanical preparation of extracted human teeth, with samples collected in time intervals of 12 h, 1, 2 and

3 days after instrumentation. The results demonstrated greater antimicrobial substantivity of 2 % CHX compared with 1 % and 0.1 % concentrations for 3 days. Rosenthal, Spangberg, and Safavi⁹ (2004) evaluated the substantivity of CHX in root canal systems and the length of time this effect persisted. Bovine roots remained in CHX for 10 min and were evaluated in time intervals of 1 day, 3, 6 and 12 weeks using UV spectrophotometry at 253 nm. The results showed that CHX was retained in radicular dentin and had an antimicrobial effect for 12 weeks, although this effect became reduced over time.

In the present study, Raman spectroscopy suggested the presence of CHX in radicular dentin by revealing a shift in the peak corresponding to the HA in the group CHX since the non-vital teeth could not undergo mineralisation, thereby discarding a spectral change resulting from the occurrence of carbonation in HA, which would lead to the same spectral change. Jones et al. 34 (2000) evaluated the effects of polymeric components (polycarbophil, polyvinylpyrrolidone and hydroxymethyl cellulose) on the physical state of CHX within semi-solid bioadhesive formulations by using Raman spectroscopy. The results showed that there was a change in the most intense band, with a wavenumber shift from ~1,564 cm⁻¹ to ~1,608 cm⁻¹ in formulations containing CHX and polycarbophil (PC), which could be attributed to the protonation of CHX by the numerous groups of carboxylic acids of PC. Pascon et al.40 (2012) evaluated the morphological and biochemical changes in pulp chamber dentin after the use of endodontic irrigants by means of the Fourier-transform (FT) Raman technique. The results demonstrated significant differences in the integrated areas of the phosphate HA peak at ~960 cm⁻¹ between the groups without treatment: 2 % CHX; 2 % CHX + 17 % EDTA; 17 % EDTA; 5.25 % NaOCl and 5.25 % NaOCl + 17 % EDTA, and that CHX was the irrigant that caused the greatest modifications in inorganic components. The authors justified that CHX is a cationic component with the ability to bind to anionic molecules such as phosphate HA present in the dentinal calcium-carbonate complex, which could lead to the release of small quantities of calcium from dentin.

CHX contains two positive charges in its guanidine groups, and these groups may be electrostatically attracted and bind to the phosphate group in HA by protonation ^{12,41}. This could lead to a change in the polarizability of HA and, consequently, a change in the Raman spectrum by band shifting. CHX bond to phosphate leads to the release of small quantities of calcium from dentin, which could cause changes in the Ca/P ratio of dentin⁴⁰. In this case, changes would occur in the ratio between the peaks at ~960 and ~1,070 cm⁻¹; this fact was not evaluated in the present study.

Our results showed the shift of the peak ~960 cm⁻¹ to the right in the time interval t=0 in the CHX group and the return to the initial value during the experimental periods (p < 0.05). The interaction of CHX with dentin is consistent with adsorption, instead of the reactive process

with precipitation of CHX salts⁴², which would justify the findings presented in this study with reference to the reversal of the adsorption process by the return of the peak to its previous position. This fact was not observed in the Group CHX + Water until 48 h, which suggested that the water could have influenced polarizability at 72 h. The shift of the peak at $^{\sim}960~\text{cm}^{-1}$ to lower wavenumber in 7 days was characteristic of the basification of HA by H⁺, which means a change in the polarisation or, less probably, the release of calcium of the carbonation of HA.

The PCA technique, which has been used previously with Raman spectroscopy ²² to identify changes in the composition of biological tissues due to the application of treatment/healing based on low-level laser light, is a tool that is sensitive to small spectral changes induced by changes in the chemical environment.

CONCLUSION

This study demonstrated that Raman spectroscopy and PCA effectively identified spectral changes in root dentin resulting from the adsorption of CHX after irrigation. The findings indicate that the presence of CHX modifies the polarizability of the HA phosphate groups, as evidenced by the shift to the right of the phosphate characteristic peak at ~960 cm⁻¹. This shift varies depending on the duration of the root canal's contact with CHX and the specific irrigation protocol used (CHX alone versus CHX followed by rinse with distilled water).

These spectral alterations suggest that the interaction between CHX and dentin occurs through reversible protonation processes, which can be further influenced by the presence of water, thereby altering the behaviour of the characteristic peak. Moreover, the application of PCA enabled the discrimination of subtle chemical changes induced by the irrigant, highlighting its potential as a complementary tool for evaluating endodontic treatment protocols.

Combining Raman spectroscopy and multivariate analysis can unleash the possibility of monitoring chemical changes in dentin non-invasively. This approach could significantly optimise endodontic treatments by refining irrigation protocols and enhancing antimicrobial efficacy without compromising the structural integrity of dentin.

ACKNOWLEDGMENTS

The authors gratefully acknowledge the Federal University of Bahia for financial support on this project.

REFERENCES

- 1. Gulabivala K, Ling Ng Y. Factors that affect the outcomes of root canal treatment and retreatment A reframing of the principles. Int Endod J. 2023; 56(Suppl. 2):82-115. doi:10.1111/iej.13897
- 2. Fransson H, Dawson V. Tooth survival after endodontic treatment. Int Endod J. 2023;56(Suppl. 2):140-53. doi:10.1111/iej.13835
- 3. Siqueira Junior JF, Rôças IN, Marceliano-Alves MF, Pérez AR, Ricucci

- D. Unprepared root canal surface areas: causes, clinical implications, and therapeutic strategies. Braz Oral Res. 2018; 32(Suppl.1):e65-e83. doi:10.1590/1807-3107bor-2018.vol32.0065
- 4. Espir GC, Nascimento-Mendes CA, Guerreiro-Tanomaru JM, Freire LG, Gavini G, Tanomaru-Filho M. Counterclockwise or clockwise reciprocating motion for oval root canal preparation: a micro-CT analysis. Int Endod. 2018;51(5):541-8. doi:10.1111/iej.12776
- 5. Maciel Filho MD, Zotarelli-Filho IJ. Main predictors of root canal endodontical treatment: Systematic review. Int J Dentistry Oral Sci. 2018;5(2):595-600. doi:10.19070/2377-8075-18000116
- 6. Zandi H, Petronijevic N, Mdala I, Kristoffersen AK, Enersen M, Rôças IN. Outcome of endodontic retreatment using 2 root canal irrigants and influence of infection on healing as determined by a molecular method: a randomized clinical trial. J Endod. 2019;45:1089-98. doi:10.1016/j. joen.2019.05.021
- 7. Ruksakiet K, Hanák L, Farkas N, Mikó A, Varga G, Lohinai Z. Antimicrobial efficacy of chlorhexidine and sodium hypochlorite in root canal disinfection: a systematic review and meta-analysis of randomized controlled trials. J Endod. 2020;46(8):1032-41.e7. doi:10.1016/j. joen.2020.05.002
- 8. Oncu A, Celikten B, Aydin B, Amasya G, Tuncay E, Eskiler GG, Açik L. Antibacterial efficacy of silver nanoparticles, sodium hypochlorite, chlorhexidine, and hypochlorous acid on dentinal surfaces infected with Enterococcus faecalis. Microsc Res Tech. 2024;87:2094-102. doi:10.1002/jemt.24590
- 9. Rosenthal S, Spangberg L, Safavi K. Chlorhexidine substantivity in root canal dentin. Oral Surg. Oral Med Oral Pathol Oral Radiol Endod. 2004;98:488-92. doi:10.1016/j.tripleo.2003.07.005
- 10. Misra DN. Interaction of chlorhexidine digluconate with and adsorption of chlorhexidine on hydroxyapatite. J Biomed Mater Res. 1994;28:1375-81. doi:10.1002/jbm.820281116
- 11. Weissheimer T, Pinto KP, Silva EJNL da, Hashizume LN, Rosa RA da, Só MVR. Disinfectant effectiveness of chlorxidine gel compared to sodium hypochlorite: a systematic review with meta-analysis. Restor Dent Endod. 2023; 48(4):e38. doi:10.5395/rde.2023.48.e37
- 12. Tartari T, Wichnieski C, Bachmann L, Jafelicci Junior M, Silva RM, Letra A, et al. Effect of the combination of several irrigants on dentine surface properties, adsorption of chlorhexidine and adhesion of microorganisms to dentine. Int Endod J. 2018;51:1420-33. doi:10.1111/iej.12960
- 13. Chandki R, Nikhil V, Kalyan SS. Comparative evaluation of substantivity of two biguanides 0.2% polyhexanide and 2% chlorhexidine on human dentin. J Conserv Dent. 2020;23:46-50. doi:10.4103/JCD. JCD_256_19
- 14. Souza M, Cecchin D, Farina AP, Leite CE, Cruz FF, Pereira CC, et al. Evaluation of chlorhexidine substantivity on human dentin: A chemical analysis. J Endod. 2012;38:1249-52. doi:10.1016/j.joen.2012.06.003
- 15. Mahendra A, Koul M, Upadhyay V, Rahul D. Comparative evaluation of antimicrobial substantivity of different concentrations of chlorhexidine as a root canal irrigant: an in vitro study. J Oral Biol Craniofac Res. 2014;4:181-5. doi:10.1016/j.jobcr.2014.11.005
- 16. Hanlon EB, Manoharan R, Koo TW. Prospects for in vivo Raman spectroscopy. Phys Med Biol. 2000;45:1-59. doi:10.1088/0031-9155/45/2/20
- 17. Cheng JX, Xie XS. Vibrational spectroscopic imaging of living systems: An emerging platform for biology and medicine. Science 2015;350(6264):aaa8870. doi:10.1126/science.aaa8870

- 18. Berger AJ, Koo TW, Itzkan I, Horowitz G, Feld MS. Multicomponent blood analysis by near-infrared Raman spectroscopy. Appl Opt. 1999;38:2916-26. doi:10.1364/ao.38.002916
- 19. Saatkamp CJ, Almeida ML de, Bispo JA, Pinheiro ALB, Fernandes AB, Silveira L. Quantifying creatinine and urea in human urine through Raman spectroscopy aiming at diagnosis of kidney disease. J Biomed Opt. 2016;21(3):37001. doi:10.1117/1.JBO.21.3.037001
- 20. Silveira FL, Pacheco MT, Bodanese B, Pasqualucci CA, Zângaro RA, Silveira L. Discrimination of non-melanoma skin lesions from non-tumor human skin tissues in vivo using Raman spectroscopy and multivariate

statistics. Lasers Surg Med. 2015;47(1):6-16. doi:10.1002/lsm.22318

- 21. Lopes CB, Pinheiro AL, Sathaiah S, Da Silva NS, Salgado MAC. Infrared laser photobiomodulation (lambda 830 nm) on bone tissue around dental implants: A Raman Spectroscopy and Scanning Electronic Microscopy study in rabbits. Photomed. Laser Surg. 2007;25(2):96-101. doi:10.1089/pho.2006.2030
- 22. Souza RA, Xavier M, Mangueira NM, Santos AP, Pinheiro ALB, Villaverde AB, et al. Raman spectroscopy detection of molecular changes associated with two experimental models of osteoarthritis in rats. Lasers Med Sci. 2014;29(2):797-804. doi:10.1007/s10103-013-1423-1
- 23. Castro ICV de, Rosa CB, Dos Reis Júnior JA, Moreira LGP, Aragão JS, Barbosa AF dos S, et al. Assessment of the use of LED phototherapy on bone defects grafted with hydroxyapatite on rats with iron-deficiency anemia and nonanemic: a Raman spectroscopy analysis. Lasers Med Sci. 2014;29(5):1607-15. doi:10.1007/s10103-014-1562-z
- 24. Gamsjäger S, Zoehrer R, Roschger P, Fratzlb P, Klaushofera K, Mendelsohnc R, et al. Vibrational spectroscopy in biomedical science: bone. Proc SPIE. 2009; 7166:716602. doi:10.1117/12.807914
- 25. Cárcamo JJ, Aliaga AE, Clavijo RE, Brañes MR, Campos-Vallette MM. Raman study of the shockwave effect on collagens. Spectrochim Acta A Mol Biomol Spectrosc. 2012;86:360-5. doi:10.1016/j.saa.2011.10.049
- 26. Breschi L, Maravic T, Comba A, Cunha SR, Loguercio AD, Reis A, et al. Chlorhexidine preserves the hybrid layer in vitro after 10-years aging. Dent Mater. 2020;36(5):672-80. doi:10.1016/j.dental.2020.03.009
- 27. Movasaghi Z, Rehman S, Rehman IU. Raman spectroscopy of biological tissues. Appl Spectrosc Rev. 2007;42:493-541. doi:10.1080/05704920701551530
- 28. Timlin JA, Carden A, Morris MD. Chemical microstructure of cortical bone probed by Raman transects. Appl Spectrosc. 1999;53(11):1429-35. doi:10.1366/00037029919457
- 29. Awonusi A, Morris MD, Tecklenburg MMJ. Carbonate assignment and calibration in the Raman spectrum of apatite. Calcif Tissue Int. 2007;81:46-52. doi:10.1007/s00223-007-9034-0
- 30. Kozielski M, Buchwald T, Szybowicz M, Baaszczak Z, Piotrowski A, Ciesielczyk B. Determination of composition and structure of spongy bone tissue in human head of femur by Raman spectral mapping. J Mater Sci Mater Med. 2011; 22(7):1653-61. doi:10.1007/s10856-011-4353-0
- 31. Scheetz BE, White WB. Vibrational spectra of the alkaline earth double carbonates. Am Min. 1977;62(1-2):36-50.
- 32. Akram Z, Aati S, Ngo H, Fawzy A. pH-dependent delivery of chlorhexidine from PGA grafted mesoporous silica nanoparticles at resin-dentin interface. J Nanobiotechnology. 2021;19(1):43-59. doi:10.1186/ s12951-021-00788-6

Assessment of the spectral changes in root dentin after irrigation with chlorhexidine: a Raman spectroscopy study

- 33. Lin S.-Y, Li M.-J, Cheng W.-T. FT-IR and Raman vibrational microspectroscopies used for spectral biodiagnosis of human tissues. J Spectroscopy. 2007;21:1-30. doi:10.1155/2007/278765
- 34. Jones DS, Brown AF, Woolfson AD, Dennis AC, Matchett LJ, Bell SE. Examination of the physical state of chlorhexidine within viscoelastic, bioadhesive semisolids using raman spectroscopy. J Pharm Sci. 2000;89(5):563-71. doi:10.1002/(SICI)1520-6017(200005)89:5<563::AI-D-JPS1>3.0.CO;2-Q
- 35. Calinescu M, Negreanu-Pirjol T, Calinescu O, Georgescu R. Spectral and biological characterization of some copper (II) complex compounds with chlorhexidine. Rev Chim. (Bucharest) 2012;63(7):682-7.
- 36. Bispo JA, De Sousa Vieira EE, Silveira Jr L, Fernandes AB. Correlating the amount of urea, creatinine, and glucose in urine from patients with diabetes mellitus and hypertension with the risk of developing renal lesions by means of Raman spectroscopy and principal component analysis. J Biomed Opt. 2013; 18(8):870-4. doi:10.1117/1.JBO.18.8.087004
- 37. Posner AS. The structure of bone apatite surfaces. J Biomed Mater Res. 1985; 19(3):241-50. doi:10.1002/jbm.820190307
- 38. Bengtsson A, Sjöberg S. Surface complexation and proton-promoted dissolution in aqueous apatite systems. Pure Appl Chem. 2009;81(9):1569-84. doi:10.1351/PAC-CON-08-10-02

- 39. Dorozhkin SV. Dissolution mechanism of calcium apatites in acids: a review of literature. World J Methodol. 2012;2(1):1-17. doi:10.5662/wim.v2.i1.1
- 40. Pascon FM, Kantovitz KR, Martin A, Puppin-Rontano R. Morphological and chemical changes in dentin after using endodontic agents: fourier transform Raman spectroscopy, energy-dispersive x-ray fluorescence spectrometry, and scanning electron microscopy study. J Biomed Opt. 2012;17(7):075008. doi:10.1117/1.JBO.17.7.075008
- 41. Nishitani Y, Hosaka K, Hoshika T, Yoshiyama M, Pashley DN. Effects of chlorhexidine in self-etching adhesive: 24 hours results. Dent Mater J. 2013; 32(3):420-4. doi:10.4012/dmj.2012-199
- 42. Souza CAS de, Colombo APV, Souto RM, Silva-Boghossian CM, Granjeiro JM, Alves GG, et al. Adsorption of chlorhexidine on synthetic hydroxyapatite and in vitro biological activity. Colloids Surf B. Biointerfaces. 2011;87(2):310-8. doi:10.1016/j.colsurfb.2011.05.035

Submetido em 03/02/2024 Aceito em 11/03/2025